Dynamics of Probe Particles in Polymer Solutions and Gels

Mitsuhiro Shibayama* and Yoshinori Isaka

Department of Polymer Science and Engineering, Kyoto Institute of Technology, Matsugasaki, Sakyo-ku, Kyoto 606-8585, Japan

Yasuhiro Shiwa

Division of Natural Science, Kyoto Institute of Technology, Matsugasaki, Sakyo-ku, Kyoto 606-8585, Japan

Received March 19, 1999

ABSTRACT: The dynamics of polystyrene probe particles in poly(*N*-isopropylacrylamide) solutions and in gels has been investigated by dynamic light scattering. Two modes, i.e., the translational diffusion of probe particles and the cooperative diffusion of polymer chains, were successfully decomposed from CONTIN analysis. The characteristic decay time of probe particles in polymer solutions became larger by a few orders of magnitude than in water. On the other hand, in the case of polymer gels, the translational diffusion of probe particles was substantially frozen, and only the cooperative diffusion of polymer networks was observed. This probe scattering method clearly demonstrates the difference in the dynamics of polymer solutions and gels. The nonergodic nature of polymer networks is also discussed with the characteristic decay time distribution function.

Introduction

Dynamic light scattering has been extensively employed in order to elucidate the dynamics of complex fluids, such as micellar solutions, glasses, and gels.[1] The dynamics of chain molecules in polymer solutions and in gels becomes cooperative above the chain overlap concentration.[2] In other words, because of transient entanglements and/or permanent cross-links, the polymer system becomes a huge "network" characterized by its mesh size of ξ. To investigate such a network structure, it is useful to examine the dynamics of probe particles embedded in the network. Such a "probe scattering" technique has been applied to study polymer solutions for more than two decades.[3−8] One of the main issues of the probe scattering lies in the discussion of variation of the translational diffusion coefficient of probe particles, D_{probe}, by varying their environment, such as the kind and/or the molecular weight of the environment polymers. Deviations from the Stokes−Einstein law were also discussed when the viscosity of the matrix was known.[5,6] The advantage of the probe scattering method is to make use of (1) strong scattering from probe particles and (2) high sensitivity to the local surroundings as revealed by a change of relaxation rate. Since the probe scattering is very sensitive to the environment of the probe particles, it has been quite successful to discuss the quality of the polymer solution and the interaction between the solvent polymers and the probes.

The probe scattering technique has also been used to study the dynamics of gels.[9−11] For instance, Allain et al.[9] focused on the dynamics of polystyrene particles in polyacrylamide during the course of gelation reaction. They found a broadening of the distribution of the relaxation rate and a departure from a single-exponential behavior at the gelation threshold. Reina et al.[11] showed that the crossover from diffusive to nondiffusive behavior depends on the length scale over which the movement of probe particles was probed. However, the following facts should be noted: probe dynamics is more complicated in the gel phase than in semidilute solutions because the movement of the particles is influenced not only by the viscosity but also by the viscoelastic effect of the network. Hence, a conventional analysis, such as a double-exponential function fitting, cannot accurately discriminate between the cooperative diffusion of the network (to be referred to as "gel mode" in this paper) and the translational diffusion of probe particles due to their coupled movement. Another important issue to study gels is the "nonergodicity".[12] In 1989, Pusey and van Megen introduced this important concept to describe the statistics for frozen structures, such as glasses and gels.[12] Hence, the scattered intensity from a gel depends on the sample position, and the contribution of an uninteresting scattering component becomes significant.[13] Owing to this concept, studies on gels have been greatly advanced.[14−16] Solidlike aspects of gels, such as spatial inhomogeneities, can be observed as a speckle pattern, i.e., a strong scattered intensity variation with the sample position.[17] Therefore, probe scattering from gels has to be examined by taking account of this effect.

In this work, we discuss the dynamics of polymer solutions and gels with and without polystyrene latex by using the distribution function of characteristic decay time, $P(\Gamma^{-1})$, where Γ^{-1} is the characteristic decay time. First, the probe diffusion for polymer solutions will be analyzed as a function of polymer concentration. Second, it will be demonstrated that (1) the two modes, i.e., the gel mode of the network (or entangled) chains and the translational diffusion mode of probe particles, can be clearly resolved in $P(\Gamma^{-1})$, and (2) cross-linking drastically changes the dynamics of polymer solutions. Finally, it will be discussed that the effect of nonergodicity becomes more significant on increasing the cross-link density.

* To whom correspondence should be addressed.

10.1021/ma990414g CCC: $18.00
Published on Web 10/01/1999

Theoretical Background

The intensity correlation function (ICF), $g^{(2)}(\tau)$, for latex solutions consisting of particles with a unimodal-size distribution is given by

$$g^{(2)}(\tau) - 1 = \exp[-2\Gamma\tau] \quad (1)$$

where τ is the time difference of photon detection, and Γ is the decay rate related to the diffusion coefficient D by

$$\Gamma = Dq^2 \quad (2)$$

where q is the magnitude of the scattering vector. The hydrodynamic radius, R_H, of latex particles is defined by the Stokes−Einstein law

$$R_H = \frac{kT}{6\pi\eta D} \quad (3)$$

where kT is the thermal energy and η is the solvent viscosity. The correlation length ξ ($\approx R_H$) is of the order of the mesh size of a polymer network and/or blob as far as the system is away from its criticality.[18]

However, in general, $g^{(2)}(\tau)$ cannot be represented by a single-exponential function given by eq 1 because of polydispersity nature of polymeric systems. To take into account such a polydispersity effect and/or multimode relaxation in ICF, a decay rate distribution function defined by

$$g^{(2)}(\tau) - 1 = [\int_0^\infty G(\Gamma) \exp(-\Gamma\tau)\, d\Gamma]^2 \quad (4)$$

is employed, where $G(\Gamma)$ is the decay rate distribution function with characteristic decay rate, Γ. Since the observable quantity is not $G(\Gamma)$ but $g^{(2)}(\tau)$, an inverse Laplace transform of $\sqrt{g^{(2)}(\tau)-1}$ is necessary to evaluate the distribution, $G(\Gamma)$.[19] Practically, the characteristic decay time distribution, $P(\Gamma^{-1})$, is more commonly used rather than $G(\Gamma)$, where $P(\Gamma^{-1})$ is defined to be $P(\Gamma^{-1}) \equiv G(\Gamma)$. Note that the peak position in $P(\Gamma^{-1})$ corresponds to R_H.

Tanaka et al. showed that $g^{(2)}(\tau)$ for polymer gels can also be described by a single-exponential function.[2] However, due to the nonergodicity, $g^{(2)}(\tau)$ becomes sample-position-dependent and is given by

$$g^{(2)}{}_p(\tau) - 1 = {\sigma_p}^2 \exp[-2D_{A,p}q^2\tau] \quad (5)$$

where ${\sigma_p}^2$ is the initial amplitude of the correlation function and the subscript p indicates sample-position dependence. More precisely, $g^{(2)}(\tau)$ is given by[14]

$$g^{(2)}{}_p(\tau) - 1 = {X_p}^2 \exp(-2Dq^2\tau) + 2X_p(1 - X_p) \times \exp(-Dq^2\tau) \quad (6)$$

where D is the cooperative diffusion coefficient of the system. The variable X_p denotes the ratio of the intensities from thermal fluctuations, I_F, to the total intensity, I_p, at a given sample position, p, and is given by

$$X_p = I_F/I_p \quad (7)$$

By evaluating $D_{A,p}$ at many sample positions as a function of I_p, one can evaluate D and the thermal component, I_F, with the following relationship

$$D = \frac{D_A}{2 - X_p} = \frac{D_A}{2 - I_F/I_p} \quad (8)$$

Because $0 < X \leq 1$, the D_A is limited in the range of $D/2$ (pure heterodyne mode) $< D_A \leq D$ (pure homodyne mode).

Experimental Section

Sample. (1) Polymer Solutions. Two series of *N*-isopropylacrylamide (NIPA) polymer solutions (PNIPA) were prepared by redox polymerization in distilled water with and without polystyrene latex. The monomer concentrations of NIPA, C, were chosen to be 100, 150, 200, 300, and 400 mM.[20] The initiator concentration (ammonium persulfate) was fixed to be 1.75 mM. These monomers and reagents were dissolved in distilled water and degassed. After chilling the mixture solutions in a refrigerator for about 30 min, 8 mM tetramethylethylenediamine was added and the polymerization/gelation was initiated. The gelation was conducted in a 10 mm glass test tube at 20 °C. The concentration of the latex, i.e., polystyrene latex, with diameter of 850 ± 50 Å (Cosmobio Chem., Co., Japan) was adjusted such that its scattered intensity was about 4×10^4 Hz at the scattering angle of 90°.

(2) Gels. NIPA gels were prepared by the same method as described above except for addition of cross-linker, i.e., *N*,*N*′-methylenebis(acrylamide) (BIS). The cross-linker concentration, C_{BIS}, was varied from 0, 0.5, 1.25, 1.0, 1.5, 2.0, 4.31, 6.0 to 8.62 mM, while C was fixed to be 200 mM. Again, two types of gels, with and without polystyrene latex, were prepared.

Viscosity Measurement. The viscosities of PNIPA aqueous solutions, prepared with C = 60, 88, 100, 150, and 200 mM NIPA monomer solutions, were measured as a function of polymer concentration, C_{polym}, with a Ubbelohde capillary viscometer at 20 ± 0.05 °C. The time required for the solution to pass the two meniscuses of the viscometer was recorded, which is proportional to the viscosity. A typical time was a few hundred seconds and was very reproducible with an error less than ±0.1 s. Therefore, the relative error was estimated to be about 0.1%. The specific viscosity, η_{sp}, is then obtained by

$$\eta_{sp} = \frac{\eta_{soln} - \eta_0}{\eta_0} \quad (9)$$

where η_{soln} and η_0 are the viscosities of the solution and the solvent, respectively.

Dynamic Light Scattering. Dynamic light scattering (DLS) measurements were carried out on a DLS/SLS-5000 compact goniometer, ALV, Langen, coupled with an ALV photon correlator. A 35 mW helium−neon laser (the wavelength in a vacuum; λ = 6328 Å) was used as the incident beam. To obtain an ensemble average, the intensity−time correlation function, $g^{(2)}(\tau)$, was obtained at 20 different sample positions. All the measurements were carried out at 20 °C. The characteristic decay time distribution function, $P(\Gamma^{-1})$, was obtained from $g^{(2)}(\tau)$ with an inverse Laplace transform program (a constrained regularization program, CONTIN). The scattering angle was 90° unless noted otherwise, which corresponds to q = 0.0187 nm^{-1}. The details of the data analysis are discussed elsewhere.[19]

Results and Discussion

(1) Molecular Weight Characterization. Figure 1 shows the polymer concentration, C_{polym}, dependence of the reduced viscosity, $\eta_{red} \equiv \eta_{sp}/C_{polym}$, for PNIPA solutions prepared from different monomer concentrations C (= 60, 88, 100, 150, and 200 mM). Viscosity measurements for polymer solutions with higher C, i.e., C = 300 and 400 mM, could not be carried out since

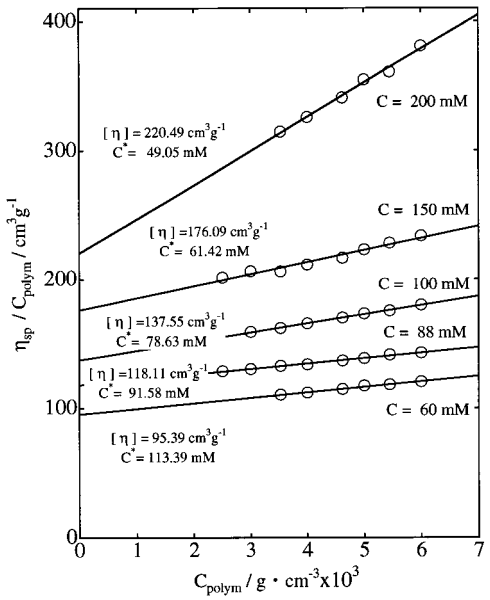

Figure 1. Polymer concentration, C_{polym}, dependence of the reduced viscosity, $\eta_{red} \equiv \eta_{sp}/C_{polym}$, for PNIPA aqueous solutions prepared from different initial monomer concentrations, C. The $[\eta]$ and C^* are the estimated intrinsic viscosity and the chain overlap concentration, respectively.

the viscosity was too high for capillary viscometry. By extrapolating η_{sp}/C_{polym} to zero concentration, the intrinsic viscosity, $[\eta]$, was estimated, i.e.,

$$[\eta] \equiv \lim_{C \to 0} \frac{\eta_{sp}}{C_{polym}} \tag{10}$$

Then, the chain overlap concentration, C^*, of PNIPA solutions was estimated with the following equations,

$$C^* = \frac{3 \times 6^{3/2}\Phi}{4\pi N_A[\eta]} \tag{11}$$

where Φ is the universal constant, and we employed the value of $\Phi = 2.1 \times 10^{23}$.[21] The values of $[\eta]$ and C^* are also shown in the figure. It is of quite importance to estimate the variation of the molecular weight of the PNIPA solutions, M, as a function of C because we deal with a series of PNIPA aqueous solutions in which M varies as a function of the monomer concentration at preparation, C. We estimated the molecular weight of our PNIPA solutions by the following relation:[22]

$$[\eta] = 0.11M^{0.51}\ \text{cm}^3/\text{g (at 20 °C)} \tag{12}$$

which is the only empirical relation available to us to the best of our knowledge. The resulting M vs C relation is shown in Figure 2. Note in eq 12 that its molecular weight exponent is very close to the value expected from theories of flexible polymers in Θ solvents. However, according to the fact that PNIPA gels are in swollen state at this temperature,[23] we believe that our PNIPA chains behave as in a good solvent. In fact, through measurement of the radius of gyration and the hydrodynamic radius, Wu and Zhou[24] concluded that the PNIPA chain in water behaves like a random coil in a good solvent at 20 °C. Therefore, in the absence of well-characterized monodisperse PNIPA in hand, we should regard eq 12 just as a means of estimating M for our samples. (This remark should be kept in mind in the

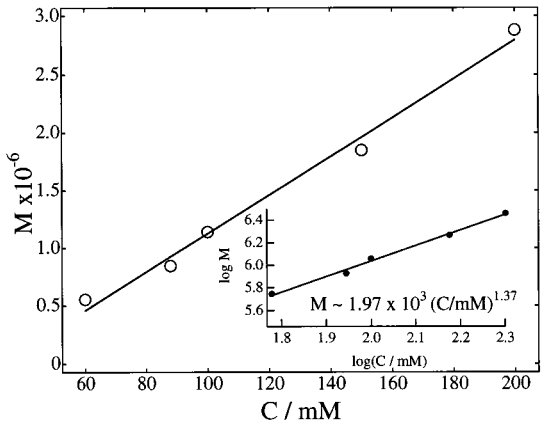

Figure 2. Initial monomer concentration (C) dependence of the molecular weight (M) of PNIPAs prepared by redox polymerization.

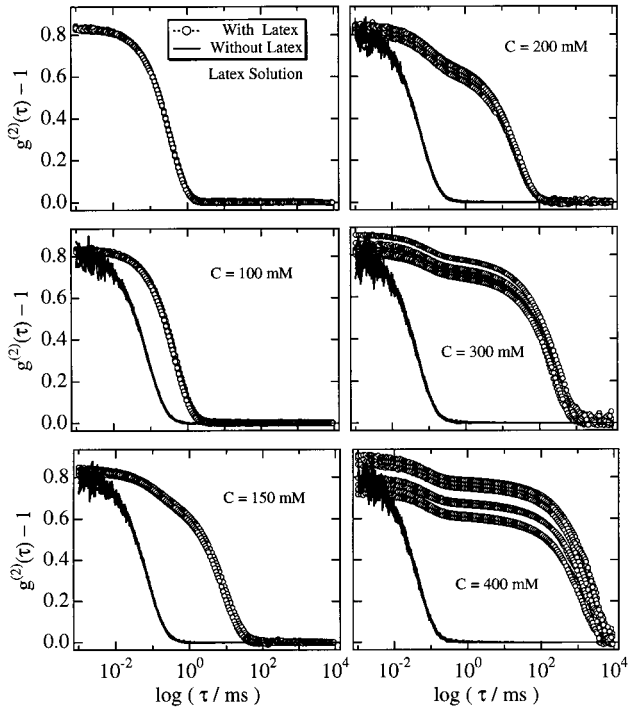

Figure 3. Series of intensity−time correlation functions (ICF), $g^{(2)}(\tau)$, for PNIPA solutions with (open circles; with latex) and without polystyrene latex (solid lines; without latex).

subsequent discussion.) Empirical equations for the estimation of M can be drawn from Figure 2 as

$$M \approx 1.97 \times 10^3 (C/\text{mM})^{1.37} \tag{13}$$

(**2**) **Polymer Solutions.** Figure 3 shows a series of intensity−time correlation functions (ICF), $g^{(2)}(\tau) - 1$, for NIPA polymer solutions with (open circles; with latex) and without polystyrene latex (solid lines; without latex). Ten ICFs out of 20 were chosen arbitrarily and plotted for each sample. C was varied from 0 to 400 mM. In the case of "without latex", each of the $g^{(2)}(\tau)$'s seems to have a single decay with $\Gamma^{-1} \approx 10^{-1}$ ms, i.e., the steep decay at $\tau \approx 10^{-1}$ ms. This decay corresponds to the cooperative diffusion of the polymer chains ("gel mode"). On the other hand, $g^{(2)}(\tau)$ for "with latex" has a clear decay of $\Gamma^{-1} \approx 10^0$ ms (translational mode), having a larger value of Γ^{-1} with increasing C. For $C \geq 150$ mM, $g^{(2)}(\tau)$ starts to have another characteristic decay $\Gamma^{-1} \approx$

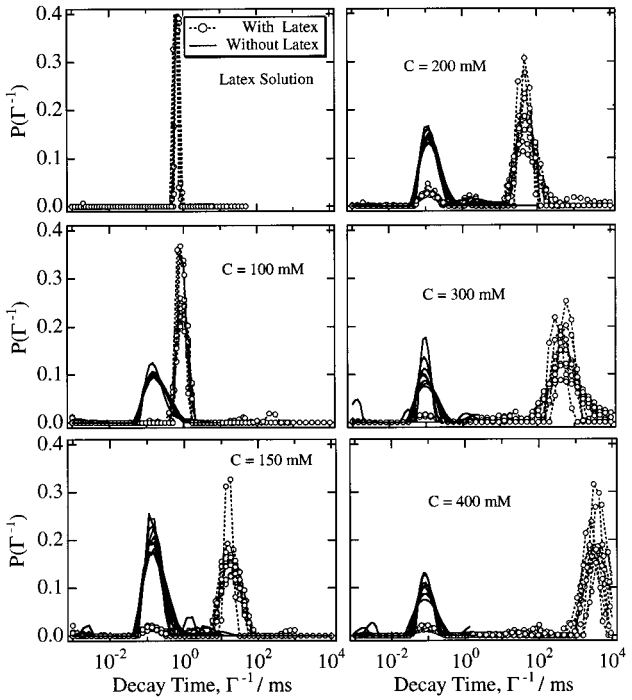

Figure 4. Series of characteristic decay time distribution functions, $P(\Gamma^{-1})$, for PNIPA solutions with (open circles; with latex) and without polystyrene latex (solid lines; without latex).

10^1 ms, which also moves toward a larger value with increasing C. The $g^{(2)}(\tau)$'s for $C \geq 200$ mM are irreducible to a single curve, indicating that $g^{(2)}(\tau)$'s are sample-position-dependent. This may suggest that the system becomes nonergodic.

Figure 4 shows a series of characteristic decay time distribution functions, $P(\Gamma^{-1})$, for PNIPA solutions with and without polystyrene latex; they have one-to-one correspondence to $g^{(2)}(\tau)$'s in Figure 3. In the case of the latex solution (without PNIPA; the top figure in the left column), a spikelike distribution is obtained at $\Gamma^{-1} \approx 10^0$ ms. This gives the diameter of the probe particle (≈850 Å). Interestingly, the peak position shifts to a larger value of Γ^{-1} by a few orders of magnitude with increasing C from 0 to 400 mM. In addition, the peak profiles become more scattered with increasing C. Contrary to this, a single peak is observed in PNIPA solutions without latex at values of Γ^{-1} smaller than those of latex solution, and the peak position is rather insensitive to C. Thus, a clear difference was observed between the two cases of matrix with and without latexes.

From the compiled data[25] for the radii of gyration, R_G, of polystyrene chains in semidilute solution in CS_2, we estimate that R_G of our PNIPA chain in semidilute regions is comparable to the size of the latex particles; for example, we estimate $R_G \approx 700$ Å for $C/C^* = 3.2$ with $M = 5 \times 10^6$. Hence, our ternary (PNIPA + PS latex + water) system may be regarded as a binary (polymer + solvent) polymer solution, at least as a first approximation. This then allows us to assign the fast-mode peak of $P(\Gamma^{-1})$ as D_{coop} and the slow mode as D_{probe}, where D_{coop} and D_{probe} are the cooperative and the translational (self-) diffusion coefficient of the non-draining polymer solutions. One might argue that our ternary system may be regarded as ternary polymer solution (polymer + polymer + solvent). However, we note that the position of the cooperative diffusion peak is not altered with the addition of latexes. On the other hand, the fast-mode diffusion coefficient in ternary polymer solutions is predicted[26] to increase with the added polymer concentration. Therefore, we preclude such an alternative interpretation.

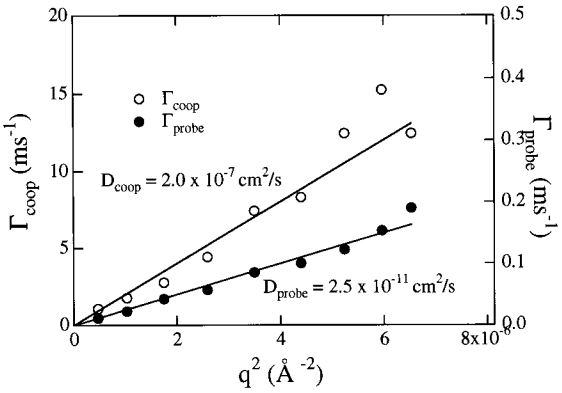

Figure 5. The q dependence of the characteristic relaxation rates, Γ_{coop} and Γ_{probe}.

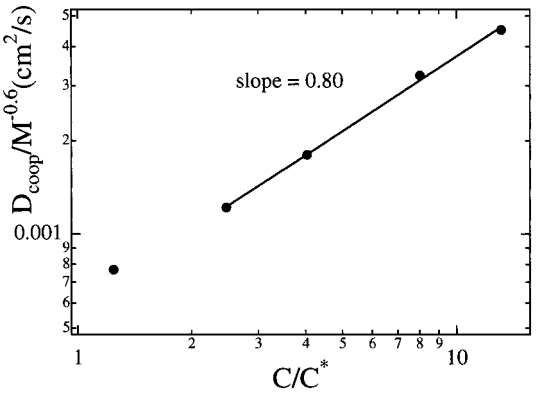

Figure 6. The C dependence of the cooperative diffusion coefficient, D_{coop}, for PNIPA solution, where C is scaled with C^*, the chain overlap concentration.

It is important to check whether these are in fact a diffusive mode or not. If it is diffusive, the characteristic rate, Γ, is proportional to q^2. In Figure 5 is shown the q^2 dependence of the relaxation rates, Γ_{coop} and Γ_{probe} for the gel mode and the probe diffusion of the polymer solution with $C = 150$ mM, respectively. The scattering angle was varied from 30° to 150°. Γ_{coop} and Γ_{probe} were evaluated from the peak positions of $P(\Gamma^{-1})$. As shown in the figure, both Γ_{coop} and Γ_{probe} increase linearly with q^2, indicating that both are diffusive modes. The diffusion coefficient, D_{coop}, obtained from the slope, is 2×10^{-7} cm^2/s. This is a typical value for PNIPA aqueous solutions in this concentration regime.[27] On the other hand, D_{probe} is estimated from Γ_{probe} to be 2.5×10^{-11} cm^2/s, which is about 1/2000 times that in water.

The concentration dependence of D_{coop} was evaluated from the diffusion peaks of PNIPA solutions without latex. Figure 6 shows the variation of D_{coop} as a function of C. Here, D_{coop} was estimated by taking average of the values of Γ^{-1} obtained at 20 different sample positions and was converted to the diffusion coefficient via eq 2. The values of M and C^* for the given PNIPA solutions were estimated with eq 12 and the relation $C^* \approx 2.02 \times 10^3 (C/\text{mM})^{-0.699}$. Since D_{coop} represents the inverse of the mesh size ξ of the entangled chains, and the ξ decreases upon increase of C, we expect an increase of D_{coop} with C. The experimental result shown in Figure 6 confirms this picture. More quantitative analysis can be made on Figure 6. According to the renormalization-

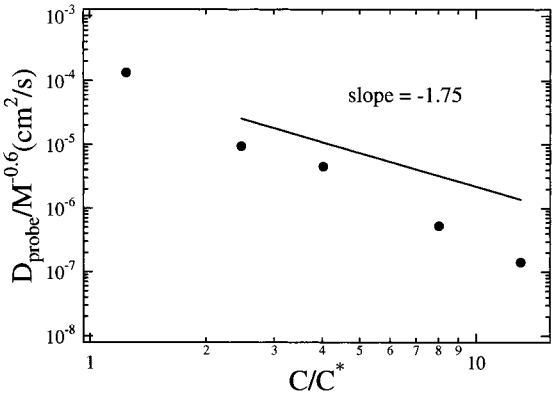

Figure 7. The C dependence of the translational diffusion coefficient of the probe particles, D_{probe}.

group (RG) treatment of dynamics of semidilute polymer solutions,[28] the ratio of D_{coop} to its dilute limit, D^0_{coop}, is a universal function of the overlap ratio C/C^*, and asymptotically ($C/C^* \to \infty$) this ratio approaches

$$D_{coop}/D^0_{coop} \sim (C/C^*)^{\nu/(3\nu - 1)} \tag{14}$$

in accord with the scaling prediction;[18] ν is the excluded-volume exponent. Assuming that our polymer solution is a good-solvent solution, we have taken $D^0_{coop} \sim M^{-\nu} = M^{-0.6}$ with $\nu = {}^3/_5$ in plotting Figure 6. This assumption is justified a posteriori because the slope ($\approx$0.80) of the line depicted in the figure is close to the scaling exponent expected for the good solvent limit, i.e., $\nu/(3\nu - 1) = 0.75$.

We now turn to the translational diffusion coefficient, D_{probe}, of the probe (latex particle). As argued above, D_{probe} can be extracted from the peak position of the slow mode in $P(\Gamma^{-1})$ for PNIPA solutions with latex. The dependence of D_{probe} on the matrix polymer concentration (C) is shown in Figure 7. As the entanglements become important, the translational diffusion of the probe particle gets progressively hindered, so that D_{probe} decreases as C increases. In fact, the RG theory[28] predicts that

$$D_{probe}/D^0_{probe} \sim (C/C^*)^{(\nu - 2)/(3\nu - 1)} \tag{15}$$

as $C/C^* \to \infty$, where D^0_{probe} is the dilute limit of D_{probe}. The apparent deviation of the data points from the line with the slope $= (\nu - 2)/(3\nu - 1) = -{}^7/_4$ might imply that the steric interaction between a hard sphere (latex) and entangled chains is stronger than the interaction between the entangled chains themselves, suggesting the stronger slowing down of the probe diffusion in the former case. This clearly indicates that to regard our system as binary polymer solution is a too simplified picture for the probe diffusion process. More theoretical efforts to elucidate the nature of probe (sphere) diffusion in semidilute polymer solutions are definitely required. In this connection, we remark that we have also tested whether a stretched-exponential form, $D_{probe}/D^0_{probe} = \exp[-\alpha(C/C^*)^{\beta}]$, as advocated in ref 4 fits the data; here α and β are scaling parameters. However, a plot of log-[log(D^0_{probe}/D_{probe})] against log(C/C^*) did not follow a straight line, contrary to the above scaling law that is predicted to hold over the whole concentration range.

Figure 8 shows the C dependence of the ensemble average scattered intensity, $\langle I \rangle_E$, for PNIPA solutions with latex (open circles) and without latex (closed circles). The $\langle I \rangle_E$ for latexes solutions without PNIPA is also shown with a dashed line. As shown here, $\langle I \rangle_E$ is greatly enhanced by adding latex to the polymer solution. On the other hand, no noticeable increase in $\langle I \rangle_E$ with C is observed in the case of PNIPA solutions. This contrasts well with the case of NIPA gels as will be discussed later.

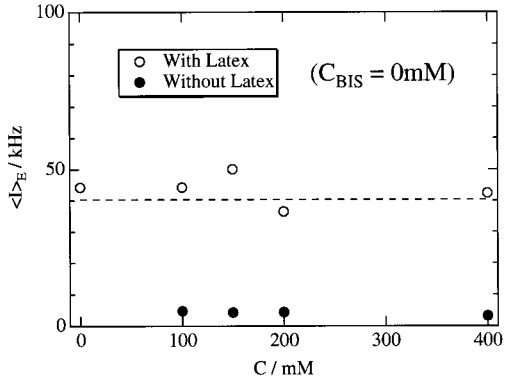

Figure 8. The C dependence of the ensemble average scattered intensity, $\langle I \rangle_E$, for PNIPA solutions "with latex" (open circles) and "without latex" (closed circles). The dashed line indicates the value of $\langle I \rangle_E$ for latex solutions without PNIPA.

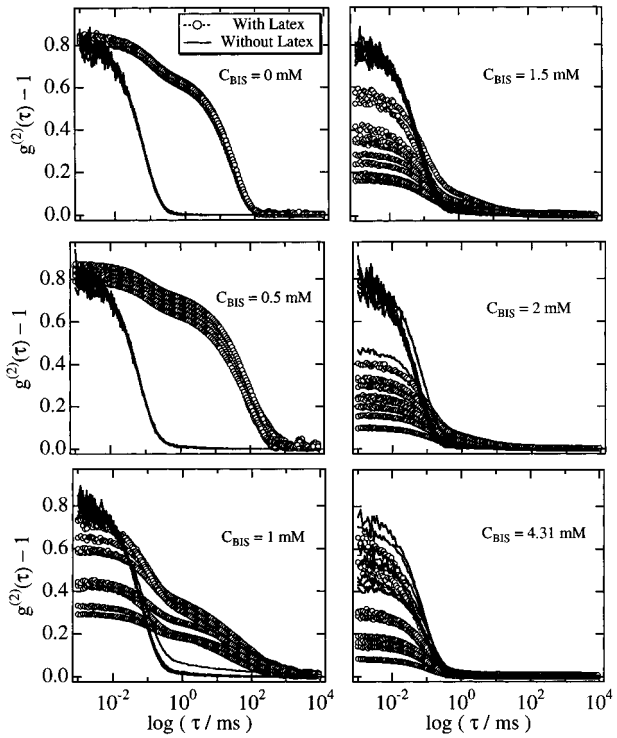

Figure 9. Series of $g^{(2)}(\tau)$'s for NIPA gels of $C = 200$ mM with (open circles; with latex) and without polystyrene latex (solid lines; without latex). The cross-linker (BIS) concentration, C_{BIS}, was varied from 0 to 4.31 mM.

(3) Polymer Gels. Figure 9 shows a series of ICFs for NIPA gels of $C = 200$ mM with (open circles; with latex) and without polystyrene latex (solid lines; without latex), where the cross-linker (BIS) concentration, C_{BIS}, was varied from 0 to 4.31 mM. Similar to the case of PNIPA solutions, $g^{(2)}(\tau)$ for "without latex" seems to have a single decay of $\Gamma^{-1} \approx 10^{-1}$ ms. However, the initial amplitude of $g^{(2)}(\tau)$, $\sigma_p{}^2$, gradually decreases with increasing C_{BIS}. The $g^{(2)}(\tau)$ for "with latex", on the other hand, has three characteristic features which become more prominent with increasing C_{BIS}: (i) double mode

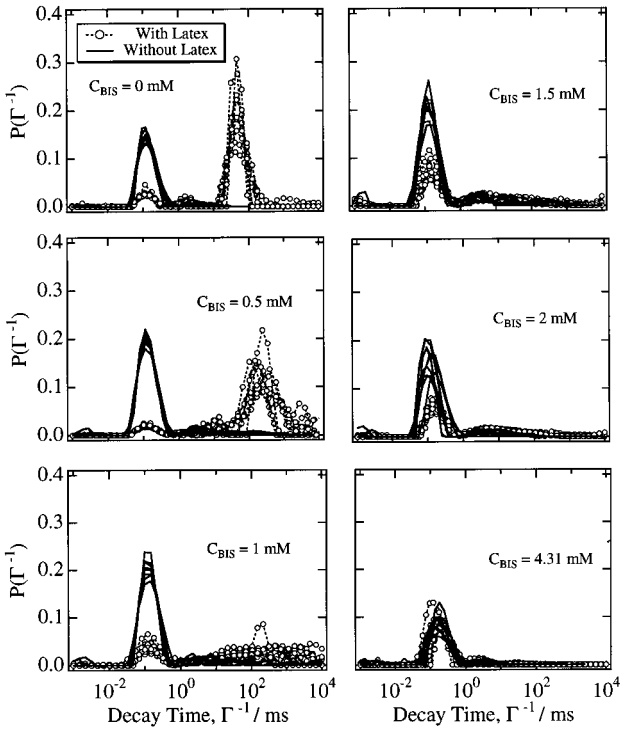

Figure 10. Series of $P(\Gamma^{-1})$'s, for NIPA gels of $C = 200$ mM with (open circles; with latex) and without polystyrene latex (solid lines; without latex). Note that the bimodal distribution is clearly seen for $C_{BIS} \leq 0.5$ mM. For $C_{BIS} \geq 1.5$ mM, only the gel mode is detected.

relaxation, (ii) strong sample-position dependence, and (iii) strong depression of σ_p^2. We now address these features one by one in the following.

Figure 10 shows a series of characteristic decay time distribution functions, $P(\Gamma^{-1})$, for NIPA gels with and without polystyrene latex, which have a one-to-one correspondence to $g^{(2)}(\tau)$'s in Figure 9. In the case of "without latex", a single mode relaxation is detected at $\Gamma^{-1} \approx 10^{-1}$ ms. This corresponds to the so-called "gel-mode" scattering. In the previous paper, we reported that the shape of $P(\Gamma^{-1})$ changes drastically with C.[27] For $C < C^*$, a single peak was observed, which indicates that the size distribution of polymer chain clusters is rather narrow. By increasing C, however, $P(\Gamma^{-1})$ had a long tail toward larger values of Γ^{-1}. The tail became longest at $C \approx C^* \approx 110$ mM,[20] which indicates a gelation threshold characteristic of cross-linked polymer solutions. For $C > C^*$, the tail became shorter with increasing C; finally $P(\Gamma^{-1})$ was reduced to a single peak function, and the gel mode was recovered. The solid curves in Figure 10 correspond to the case of $C > C^*$. Therefore, the behavior of $P(\Gamma^{-1})$'s without latex can be interpreted along this line without difficulty. The effect of cross-linker simply is a slight shift of the peak in $P(\Gamma^{-1})$.[29] On the other hand, the samples with latex exhibit a bimodal nature for $C_{BIS} < 1$ mM. This means that the DLS from polymer gels with probe particles contains two types of information, i.e., one from gel network (the peak at the smaller value of Γ^{-1}) and the other from latex particles (the peak at the larger value of Γ^{-1}). By further increasing C_{BIS} (≥ 1 mM in this particular case), however, the latter contribution is totally suppressed. This indicates that thermal motions of latex particles are completely frozen by the polymer network surrounding the particles. This behavior contrasts sharply with that of latex particles in PNIPA solution shown in Figure 4, where the thermal motions of probe particles are still allowed even at higher NIPA concentrations. This comparison clearly suggests that the presence of cross-links is fatal for the dynamics of the latex particles.

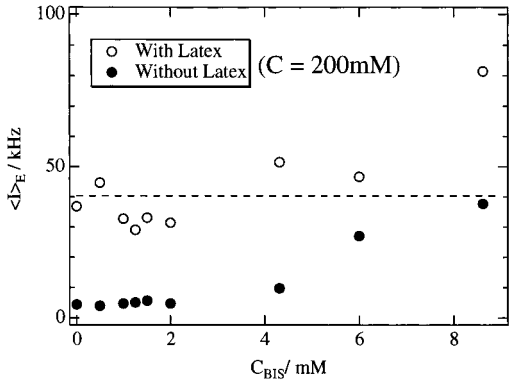

Figure 11. The C dependence of $\langle I \rangle_E$ for NIPA gels of $C = 200$ mM with latex (open circles) and without latex (closed circles). The dashed line indicates the value of $\langle I \rangle_E$ for latex solutions without NIPA gels.

It should be also noted that $P(\Gamma^{-1})$ provides information about not only the magnitude of Γ^{-1}'s but also the magnitudes of their contribution, i.e., the height of $P(\Gamma^{-1})$. For example, the peak value at $\Gamma^{-1} \approx 10^{-1}$ ms for "with latex" increases with C_{BIS}, while that at the larger Γ^{-1} ($\approx 10^2$ ms) decreases. This indicates that the trapped polystyrene particles behave as local oscillators which only contribute to an increase in $\langle I \rangle_E$ but not to the dynamics of the gel mode. Contrary to this, the gel mode characterized by the peak at $\Gamma^{-1} \approx 10^{-1}$ ms (shown with open circles) increases with C_{BIS}.

Reina et al. reported similar results to those obtained in this work.[11] However, since they used a double-exponential fit for $g^{(2)}(\tau)$, their interpretation was limited, and they could not determine whether the origin of the fast mode was the cooperative diffusion of the network (i.e., the gel mode) or the coupling between the motion of the particles and network mediated via the solvent. Our work clearly shows that (1) the fast mode corresponds to the gel mode and the slow mode is originated from the translational diffusion of the latex particles and (2) no noticeable coupling between the two takes place.

Figure 11 shows the C dependence of ensemble average scattered intensity, $\langle I \rangle_E$, for NIPA gels "with latex" (open circles) and "without latex" (closed circles). Different from the case of PNIPA solutions (Figure 8), $\langle I \rangle_E$ increases with C for both cases. This is due to an increase in the degree of inhomogeneities as discussed elsewhere.[30] Nishio et al. noted that the gel has a large interconnected space as well as many small pores (in other words, holes in mesh).[10] This also indicates the presence of spatial inhomogeneities in polymer gels.

(4) Gelation Threshold. The mesh size ξ was also estimated for the cross-linked systems from the peak position in $P(\Gamma^{-1})$ with eqs 2 and 3 as a function of C_{BIS}. However, contrary to our expectation, the mesh size ξ thus obtained increased with increasing C_{BIS}. This is simply due to nonergodicity. As discussed in the theoretical section, D_A lies between $D/2$ (pure heterodyne mode) and D (pure homodyne mode) for gels, and a simple averaging of D_A's yields deviation from D and approaches $D/2$ with increasing cross-link density. As a matter of fact, a rigorous analysis by taking account

of the nonergodicity of gels concluded that D is an increasing function of C_{BIS}[29] and that ξ decreases from 72 to 56 Å with increasing C_{BIS} from 0 (polymer solution) to 8 mM (gel). The immobilization of probe particles cannot be explained by such a small change in ξ with C_{BIS} since the size of the probe particles ($2R = 850$ Å) is much larger than ξ. Hence, it is obvious that R/ξ (= 5.9 and 7.6 for $C_{BIS} = 0$ and 8 mM, respectively) is not an essential parameter governing the dynamics of probe diffusion. The most significant factor to rule probe diffusion is whether the system has an "permanent infinite network". The symptom of infinite network formation, i.e., the gelation threshold, can be detected as a deviation of the initial amplitude of ICF, $\sigma_p^2 = g^{(2)}(\tau=0) - 1$, from unity, as extensively discussed elsewhere.[27,31] As seen in Figure 9, σ_p^2 (for "with latex") starts to be suppressed at $C_{BIS} \approx 1.0$ mM, and in fact, a more rigorous determination revealed that a gelation takes place at $C_{BIS} \approx 1.25$ mM for PNIPA prepared at $C = 200$ mM.[32] This value agrees well with the C_{BIS} value at which the probe-diffusion peak in $P(\Gamma^{-1})$ disappeared (see Figure 10).

Conclusion

The dynamics of polymer solutions and gels made of poly(*N*-isopropylacrylamide) has been investigated by dynamic light scattering of probe particles. By adding polystyrene probe particles with diameter of 850 Å, the scattered intensity was greatly enhanced. This ternary (PNIPA + PS latex + water) system could be regarded as a binary (polymer + solvent) polymer solution, and the distribution function for the characteristic decay time, $P(\Gamma^{-1})$, clearly showed the presence of two peaks originating from the cooperative gel-mode diffusion of polymer chains and the translational (self-) diffusion of the nondraining polymer solutions. It was found that addition of cross-links selectively immobilizes the translational diffusion of the probe, while the cooperative diffusion mode (i.e., the gel mode) survives. It is demonstrated that the probe dynamic light scattering coupled with the distribution function analysis is a powerful tool for (1) studies on local motions of polymer chains and/or networks in a solvent and (2) detection of the gelation threshold.

Acknowledgment. This work is partially supported by the Ministry of Education, Science, Sports and Culture, Japan (Grant-in-Aid, 09450362 and 10875199 to M.S.).

References and Notes

(1) Brown, W. *Dynamic Light Scattering, the Methods and Applications*; Clarendon Press: Oxford, 1993.
(2) Tanaka, T.; Hocker, L. O.; Benedek, G. B. *J. Chem. Phys.* **1973**, *59*, 5151.
(3) Langevin, D.; Rondelez, F. *Polymer* **1978**, *19*, 875.
(4) Phillies, G. D. J.; Brown, W.; Zhou, P. *Macromolecules* **1992**, *25*, 4948 and references therein.
(5) Pu, Z.; Brown, W. *Macromolecules* **1989**, *22*, 890.
(6) Won, J.; Onyenemezu, C.; Miller, W. G.; Lodge, T. P. *Macromolecules* **1994**, *27*, 7389.
(7) Gold, D.; Onyenemeze, C.; Miller, G. *Macromolecules* **1996**, *29*, 5700.
(8) Ye, X.; Tong, P.; Fetters, L. J. *Macromolecules* **1998**, *31*, 5785.
(9) Allain, C.; Drifford, M.; Gauthier-Manuel, B. *Polymer* **1986**, *27*, 177.
(10) Nishio, I.; Reina, J. C.; Bansil, R. *Phys. Rev. Lett.* **1987**, *59*, 684.
(11) Reina, J. C.; Bansil, R.; Konak, C. *Polymer* **1990**, *31*, 1038.
(12) Pusey, P. N.; van Megen, W. *Physica A* **1989**, *157*, 705.
(13) Sellen, D. B. *J. Polym. Sci., Polym. Phys.* **1987**, *25*, 699.
(14) Joosten, J. G. H.; McCarthy, J. L.; Pusey, P. N. *Macromolecules* **1991**, *24*, 6690.
(15) Fang, L.; Brown, W. *Macromolecules* **1992**, *25*, 6897.
(16) Panyukov, S.; Rabin, Y. *Phys. Rep.* **1996**, *269*, 1.
(17) Shibayama, M. *Macromol. Chem. Phys.* **1998**, *199*, 1.
(18) de Gennes, P. G. *Scaling Concepts in Polymer Physics*; Cornell University: Ithaca, NY, 1979.
(19) Peters, R. *Noise on Photon Correlation Functions and its Effect on Data Reduction Algorithms*; Brown, W., Ed.; Oxford University Press: Oxford, 1993.
(20) Norisuye, T.; Shibayama, M.; Nomura, S. *Polymer* **1998**, *39*, 2769.
(21) Fujita, H. *Polymer Solution*; Elsevier: Amsterdam, 1990.
(22) Kubota, K.; Fujishige, S.; Ando, I. *Polym. J.* **1990**, *22*, 15.
(23) Hirokawa, Y.; Tanaka, T. *J. Chem. Phys.* **1984**, *81*, 6379.
(24) Wu, C.; Zhou, S. *Macromolecules* **1995**, *28*, 8381.
(25) de Cloizeaux, J.; Jannink, G. *Polymer in Solution: Their Modeling and Structure*; Oxford University Press: Oxford, 1990.
(26) Borsali, R. *Light Scattering: Principles and Development*; Brown, W., Ed.; Oxford University Press: Oxford, 1996.
(27) Norisuye, T.; Takeda, M.; Shibayama, M. *Macromolecules* **1998**, *31*, 5316.
(28) Shiwa, Y. *Phys. Rev. Lett.* **1987**, *58*, 2102.
(29) Shibayama, M.; Norisuye, T.; Nomura, S. *Macromolecules* **1996**, *29*, 8746.
(30) Shibayama, M.; Takata, S.; Norisuye, T. *Physica A* **1998**, *249*, 245.
(31) Shibayama, M.; Norisuye, T.; Takeda, M. *In-situ Studies on Gelation by Dynamic and Time-Resolved Light Scattering Technique*; Stokke, B. T., Elgsaeter, A., Eds.; Wiley: New York,; Vol. 2, in press.
(32) Shibayama, M.; Takeda, M.; Norisuye, T., in preparation.

MA990414G